Monitoring respiratory and cardiac motion in CT using a continuous wave Doppler radar

Poster No.: C-2055

Congress: ECR 2013

Type: Scientific Exhibit

Authors: F. Pfanner[1], T. Allmendinger[2], T. Flohr[2], M. Kachelrieß[3]; [1]Erlangen/DE, [2]Forchheim/DE, [3]Heidelberg/DE

Keywords: Cardiac, Respiratory system, Experimental, Experimental investigations

DOI: 10.1594/ecr2013/C-2055

Purpose

To avoid motion artifacts, medical imaging devices are often synchronized to the respiratory and cardiac cycle of the patient. Today's respiratory motion monitors require additional effort in preparing the patient, such as mounting of a motion belt or the placement of an optical reflector on the patient breast [1]. Cardiac motion is typically assessed using an ECG. All these techniques have the disadvantage that additional effort in preparing the patient is needed and they are not able to measure internal organ motion without implanting markers.

Instead of using an external signal one may also estimate the motion directly from the measured data. This additional information is used to reconstruct images only from data recorded at the same cardiac or respiratory phase or by using a motion-compensated reconstruction algorithm [2]-[4]. However, this strategy requires a continuous data acquisition, also in undesired motion phases, which may be disadvantageous in therms of dose or in terms of measurement time.

An interesting alternative that does not need patient preparation is to assess the patients respiratory and cardiac motion using a continuous wave Doppler radar. The antennas can be hidden in the patient table, thus promising to be a highly convenient solution for routine use.

Methods and Materials

Doppler Radar

Figure 1 shows a simplified block diagram of the used Doppler radar. The operating frequency of 869.350 MHz is generated in the oscillator (LO). After amplifying with a power amplifier (PA), the signal is radiated on the transmit (TX) antenna. After receiving (RX) the reflected radar waves by the second antenna, the signal is mixed (MX1) with the transmitted one. Due to the fact that the two signals have the same frequency, the result of the mixer is the phase difference between the signals.

Antenna

For all measurements, we use patch antenna as shown in figure 2. In contrast to other papers [5]-[10] we use separate transmit and receive antennas. This give us a higher degree of freedom in placing the antennas. For example we can better define those points in space where the radar system should be sensitive and where not.
For our intended use, which is triggering CT scanners, the influence of the antennas onto image quality and patient dose needs to know. In particular because the antennas

and the antenna cables contain metal which can cause artifacts onto CT images [11], [12]. To test the influence of the antennas onto the CT image quality, the antennas were scanned using a clinical dual source spiral cone-beam CT system (Somatom Definition Flash, Siemens Healthcare, Forchheim, Germany). A thorax phantom was placed directly above the antennas. Figure 3 shows on of the resulting slices with two window settings. The artifacts caused by the antennas are visible only in the air window and they extend only along the long axis of the antennas. Thus these artifacts are tangent to the patient and do not influence the image quality within the patient.

Achieving a large radar-sensitive area to simplify patient positioning is done by using more antennas. To avoid the requirement for more transmit and receive units we use coax switches to switch between the antennas. Figure 4 shows the wiring between the radar unit, the coax switches and the antennas. The five antennas are arranged to have the receive antenna surrounded by the four transmit antennas.

Test Person Measurements

The system was tested using 10 test persons (6 male, 4 female). The size of the test persons range from 156 cm to 192 cm with a mean of 177 cm. Their weight ranges from 58 kg to 95 kg with a mean of 75 kg.
For the test person measurements, the radar antennas were placed on top of a standard CT table as one can see in figure 5. The test persons lie in the supine position on the table, directly above the antennas. The measurements are repeated six times having the test persons at six different positions above the antennas. At each position, two datasets were recorded: For the first acquisition, the test person was advised to normal breathing, for the second acquisition normal breathing was to be interrupted by a single deep inhale and a single deep exhale breath-hold. Each dataset has a duration of approximately 80 to 120 seconds.
As reference for the respiratory motion we used an external respiratory gating system, AZ-733V (Anzai Medical Co., LTD, Tokio, Japan), which measures the respiration by a load cell (pressure sensor) arranged with a belt on the test person. To get a reference for the cardiac motion, a standard three-lead ECG was used. All signals (radar output, Anzai system and ECG) were digitized and sent to the acquisition PC where the measurement application saves the raw data to a file.

Signal Processing

The calculation of respiratory motion from the measured radar data is done by combining the signals from all antennas using principal component analysis (PCA). PCA transposes the multidimensional input space to a single dimension by suppressing redundant information. As the respiratory motion dominates the radar signal, this signal processing step is sufficient to determine the respiratory motion from the measured radar data.
Calculation of the cardiac cycle is done by using a band pass filter which passes only spectral components in the frequency range of 40 bpm to 120 bpm. With a correlation

analysis the cardiac periodicity is determined within the filtered signal. These signal processing steps are executed with the signals from all antennas separately. In the end, the periodicity information from all antennas are overlaid to determine the heart rate and phase.

Images for this section:

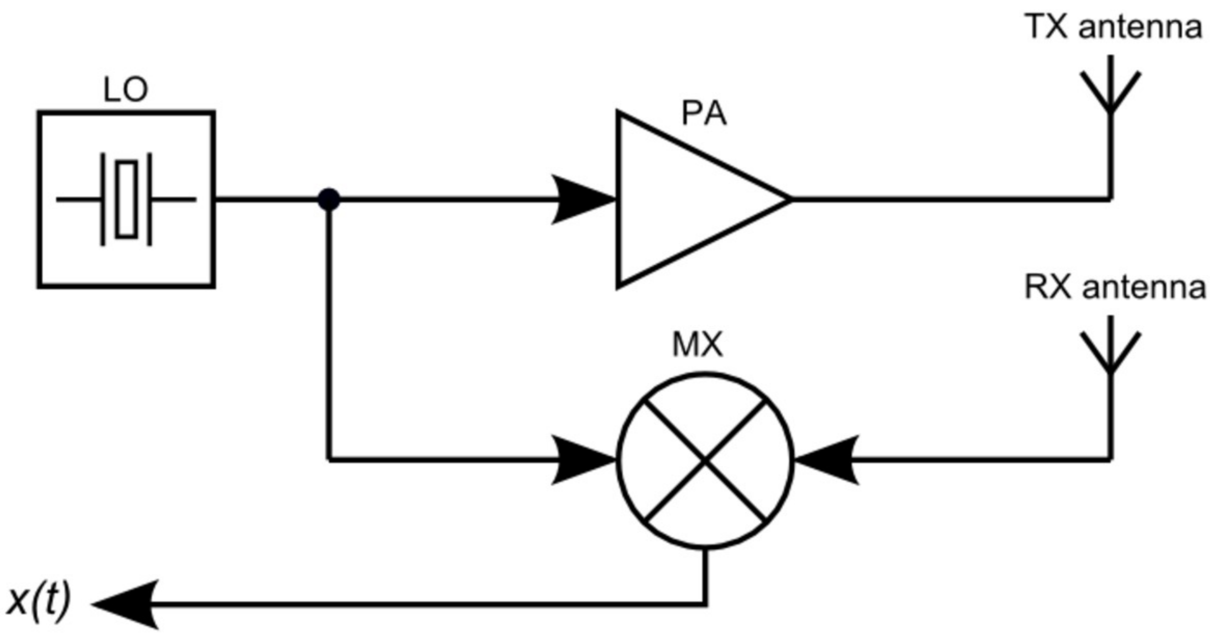

Fig. 1: Simplified block diagram of a Doppler radar

Fig. 2: Patch antenna as it is used for our measurements. Currently, we use five of these antennas; four transmit antennas and one receive antenna.

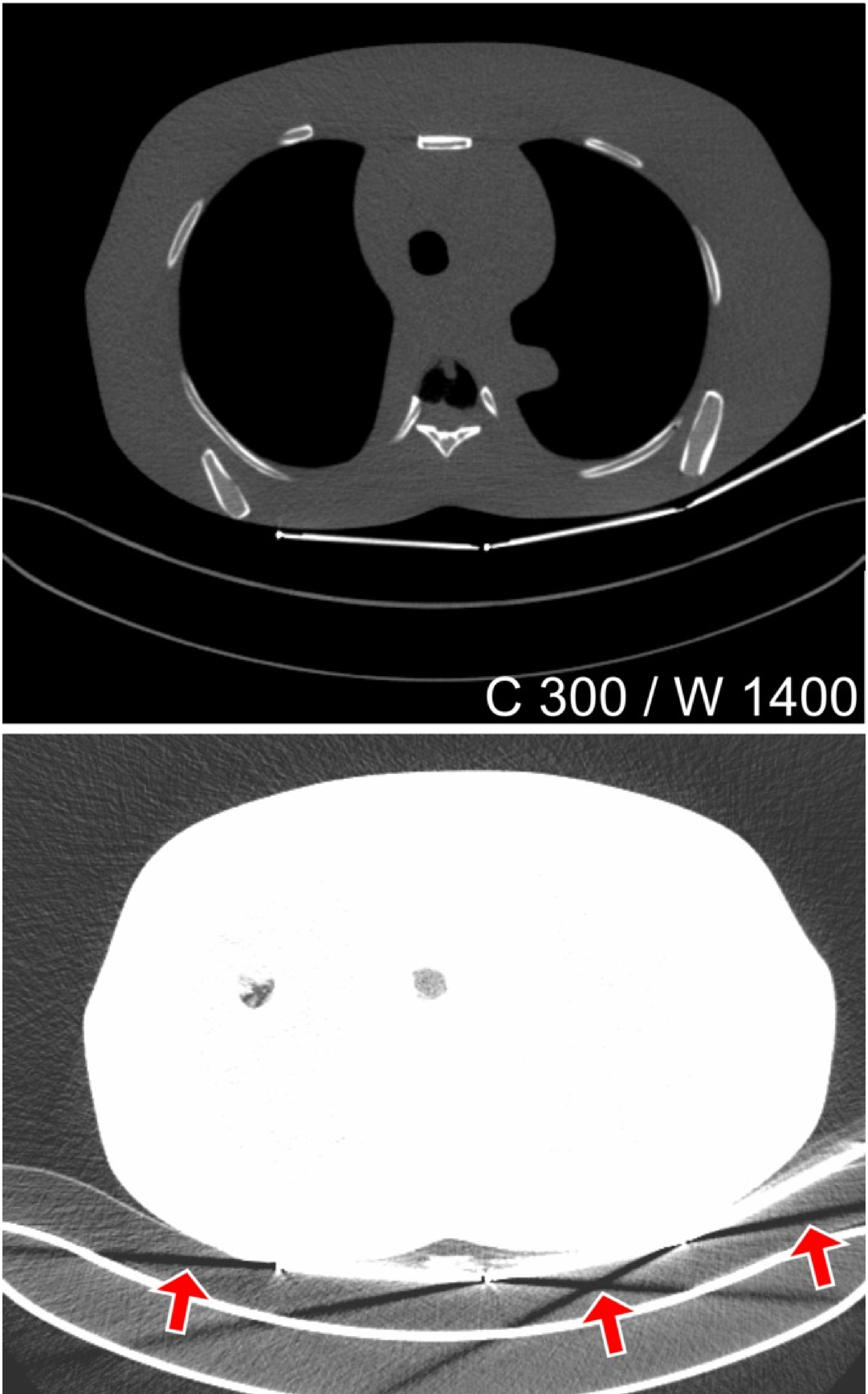
C 300 / W 1400

Fig. 3: CT images of a measured thorax phantom lying above the antennas. Both images show the same slice. Artifacts caused by the antennas extend only along the long axis of the antennas. In future applications, the antennas shall be integrated into the CT table.

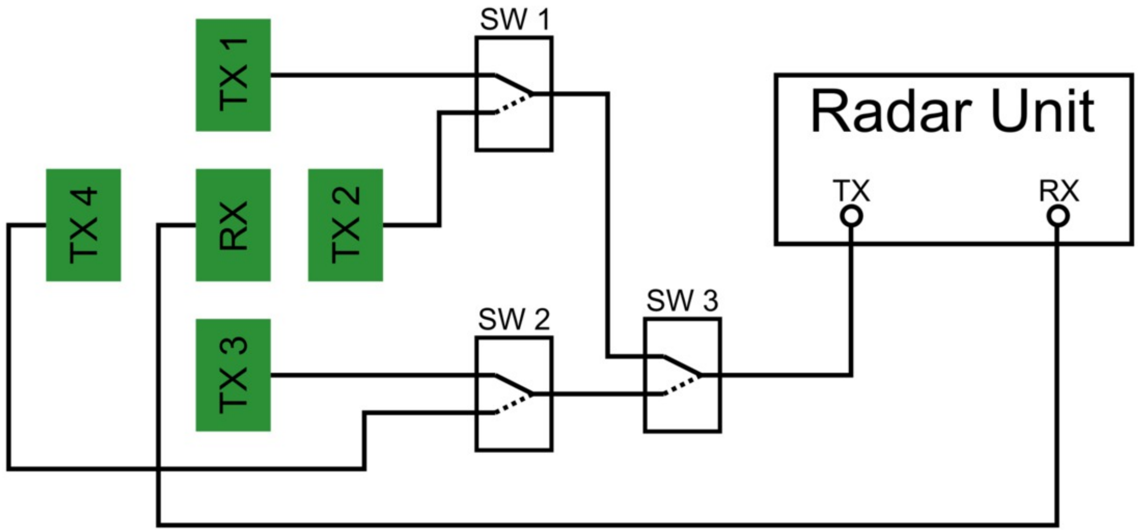

Fig. 4: Arrangement of the antennas and the connections between the radar unit, the coax switches (SW) and the antennas (green rectangles).

Fig. 5: Placement of the antennas above the CT table. The test persons rest on directly above the antennas.

Results

Respiratory Motion

Figure 6 shows a comparison between the respiratory motion measured with our radar system and the respiratory motion measured with the external respiratory gating system. Each measurement pair (radar vs. Anzai system) was compared by calculating the Pearson correlation coefficient. The mean value for this coefficient is 0.917 with a standard deviation of 0.108.

Cardiac Motion

In figure 7 the heart rate and phase determined with our radar system is shown. As one can see, the values are comparable to the heart rate and phase values determined by the ECG. For all datasets, the mean difference between the heart rate determined by our radar system and the heart rate determined with the ECG is 2.34 bpm with a standard deviation of 10.25 bpm.

Images for this section:

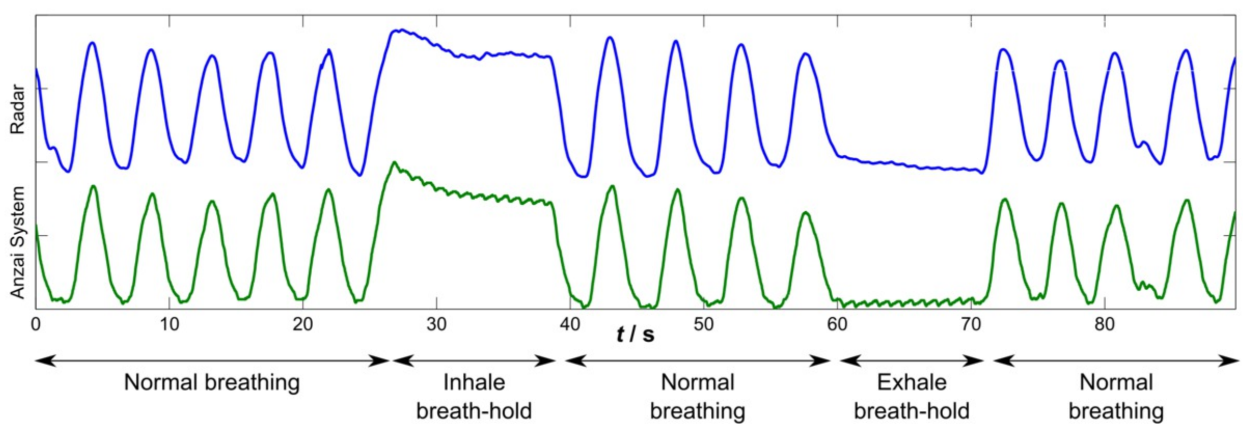

Fig. 6: Example dataset. The upper curve shows the respiratory motion measured with our radar system, the bottom curve shows the respiratory motion measured with the external respiratory gating system.

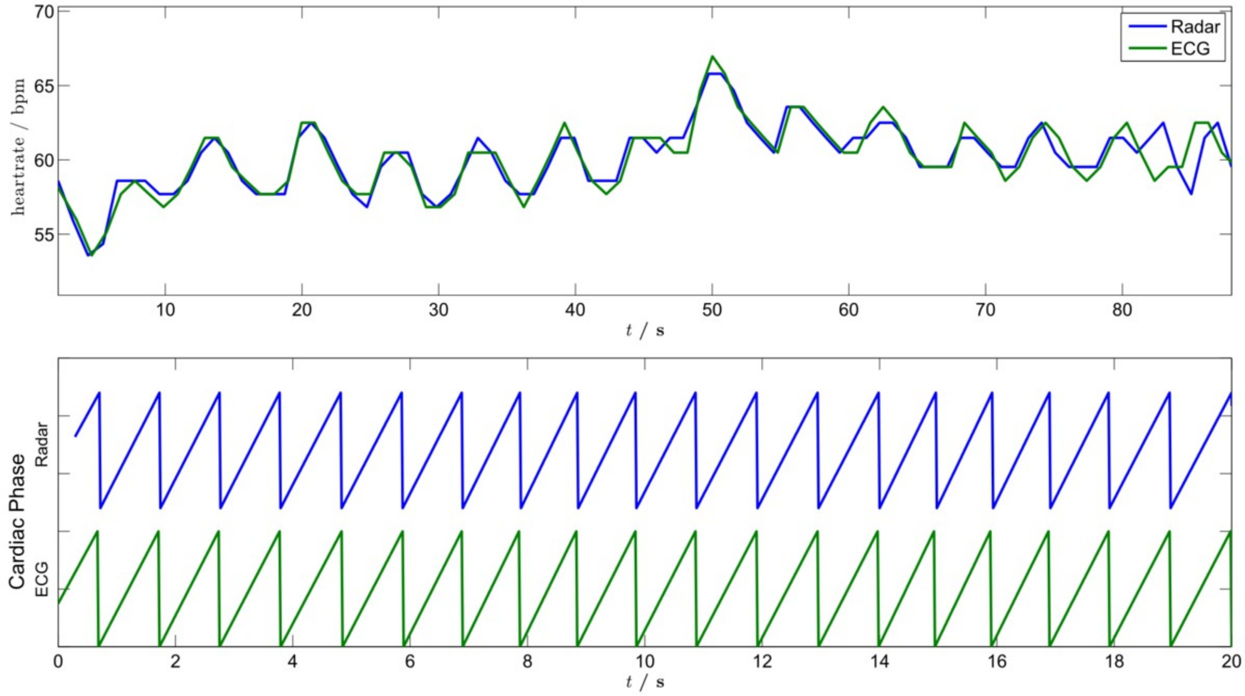

Fig. 7: Example dataset showing the heart rate and phase determined with our radar system compared to the heart rate and phase determined using ECG signals.

Conclusion

Our test person measurements indicate that the proposed radar system has the potential to detect respiratory motion quite accurately. Furthermore the preliminary results indicate that the radar system is also able to detect cardiac motion. In contrast to trigger system used today, the radar system determines these synchronization signals direct from motion inside of the body.

References

[1] S. A. Nehmeh and Y. E. Erdi, "Respiratory motion in positron emission tomography/ computed tomography: A review," Seminars in Nuclear Medicine, vol. 38, no. 3, pp. 167-176, 2008.
[2] M. Kachelrieß, D.-A. Sennst, W. Maxlmoser, and W. A. Kalender, "Kymogram detection and kymogram-correlated image reconstruction from subsecond spiral computed tomography scans of the heart," Med. Phys., vol. 29, no. 7, pp. 1489-1503, 2002.
[3] M. Buehrer, J. Curcic, P. Boesiger, and S. Kozerke, "Prospective self-gating for simultaneous compensation of cardiac and respiratory motion," Magnetic Resonance in Medicine, vol. 60, no. 3, pp. 683-690, 2008.
[4] M. Brehm, P. Paysan, M. Oelhafen, P. Kunz, and M. Kachelrieß, "Selfadapting cyclic registration for motion-compensated cone-beam CT in image-guided radiation therapy," Med. Phys., vol. 39, no. 12, pp. 7603-7618, 2012.
[5] J. Lin, "Non-invasive microwave measurement of respration," Proc. IEEE, vol. 63, p. 1530, 1975.
[6] H. J. Kim, K. H. Kim, Y. S. Hong, and J. J. Choi, "Measurement of human heartbeat and respiration signals using phase detection radar." Review of Scientific Instruments, vol. 78 (104703), no. 10, 2007.
[7] M. Varanini, P. C. Berardi, F. Conforti, M. Micalizzi, D. Neglia, and A. Macerata, "Cardiac and respiratory monitoring through non-invasive and contactless radar technique," 2008 Computers in Cardiology, vol. 35, pp. 149-152, 2008.
[8] O. Boric-Lubecke, V. M. Lubecke, I. Mostafanezhad, B.-K. Park, W. Massagram, and B. Jokanovic, "Doppler radar architectures and signal processing for heart rate extraction," Mikrotalasna revija, vol. 15, no. 2, pp. 12-17, 2009.
[9] K. Mostov, E. Liptsen, and R. Boutchko, "Medical applications of shortwave FM radar: Remote monitoring of cardiac and respiratory motion," Med. Phys., vol. 37, no. 3, pp. 1332-1338, 2010.
[10] I. Mikhelson, S. Bakhtiari, T. Elmer, and A. Sahakian, "Remote sensing of heart rate and patterns of respiration on a stationary subject using 94
GHz millimeter wave interferometry." IEEE Transactions on Biomedical Engineering, vol. 58, no. 6, pp. 1671-1677, 2011.

[11] E. Meyer, R. Raupach, M. Lell, B. Schmidt, and M. Kachelrieß, "Normalized metal artifact reduction (NMAR) in computed tomography," Med. Phys., vol. 37, no. 10, pp. 5482-5493, 2010.
[12] E. Meyer, R. Raupach, M. Lell, B. Schmidt, and M. Kachelrieß, "Frequency split metal artifact reduction (FSMAR) in computed tomography," Med. Phys., vol. 39, no. 4, pp. 1904-1916, 2012.

Personal Information

Florian Pfanner

Friedrich-Alexander-University Erlangen-Nürnberg (FAU), Erlangen, Germany

florian.pfanner@imp.uni-erlangen.de

Dr. Thomas Allmendinger

Siemens AG, Healthcare Sector, Forchheim, Germany

Dr. Thomas Flohr

Siemens AG, Healthcare Sector, Forchheim, Germany

Prof. Dr. Marc Kachelrieß

Friedrich-Alexander-University Erlangen-Nürnberg (FAU), Erlangen, Germany and German Cancer Research Center (DKFZ), Heidelberg, Germany